Characterization of a Novel Covalent Monoadduct on the RNA Overhang of an RNA−DNA Hybrid Induced by Antitumor Antibiotic Neocarzinostatin†

Ping Zheng,‡ Chuan-liang Liu,§ Zhen Xi,‡ Richard D. Smith,§ and Irving H. Goldberg*,‡

Department of Biological Chemistry and Molecular Pharmacology, Harvard Medical School, 250 Longwood Avenue, Boston, Massachusetts 02115, and Enviromental Molecular Sciences Laboratory, Mail Stop P8-19, Pacific Northwest National Laboratory, P.O. Box 999, Richland, Washington 99352

Received October 27, 1997; Revised Manuscript Received November 26, 1997

ABSTRACT: Neocarzinostatin chromophore (NCS-chrom) has been found previously to induce thiol-dependent abasic site formation and cleavage on the RNA strand of RNA−DNA hybrids. When a four-base nucleotide was deleted from the 5′ end of the DNA strand, however, an unexpected product with slow mobility, potentially a drug adduct or interstrand cross-linked material, was observed instead. End-labeling of the RNA and DNA strands showed that only the RNA strand is present in the product. The product, isolated from a denaturing polyacrylamide gel, has a fluorescence spectrum similar to that of activated NCS-chrom, and thiols with different charges give rise to products with various mobilities on the gel, indicating that the product consists of a drug adduct with NCS-chrom and thiol attached to the RNA strand of the hybrid. Mass spectroscopic (MS) analysis shows that it is a monoadduct. Chemical sequencing of 5′- and 3′-end-labeled monoadduct and MS/MS data show that drug is attached only to the U9 of the RNA in the hybrid 5′-r(CACAGAAUU9CG)/5′-d(TTCTGTG). Unlike most other DNA adducts and cross-linked products found previously, this adduct can be formed readily in the presence of atmospheric oxygen. 2′-O-Methyl and 2′-H substitutions and nucleotide replacements on the 4-base RNA overhang affect monoadduct formation to different extents, reflecting the existence of a tight three-dimensional binding pocket for the activated drug. Stability of drug adduct to heat and aniline−HOAc treatment suggests that the drug is covalently bound to the ribose of U9. Since no deuterium isotope selection effect was observed for C-1′ of U9, it is possible, although not required, that the drug abstracts H from another hydrogen source on the sugar of the targeted ribonucleotide.

The neocarzinostatin chromophore (NCS-chrom; Scheme 1, **1**), belongs to a family of highly potent enediyne antitumor antibiotics that damage duplex DNA in the presence of thiol *(1*−*3*). Form A (**1**) (Scheme 1) is the major form of NCS-chrom. Form B, the open diol decarboxylation product of form A, is present at a level of about 10% of form A *(4)*. The naphthoate moiety of NCS-chrom intercalates duplex DNA, and the rest of the molecule binds to the minor groove of DNA through hydrophobic and electrostatic interactions *(5*−*7)*. NCS-chrom activation by thiols occurs through a nucleophilic attack at C12 *(8)*, which results in the formation of the cumulene **2** *(9)*. The labile cumulene undergoes a spontaneous Bergman cyclization to the biradical **3** *(9, 10)*, which abstracts H atoms from C1′, C4′, or C5′ of the DNA duplex backbone and induces oxidative damage in the form of strand breaks and abasic sites. NCS-chrom is also able to induce site-specific cleavage at bulge sites in duplex DNA *(11, 12)*, in TAR RNA of HIV-1 *(13)*, and in RNA−DNA hybrids *(14)* in a reaction catalyzed by general base.

Scheme 1: Proposed Activation Mechanism of NCS-Chrom by Thiol

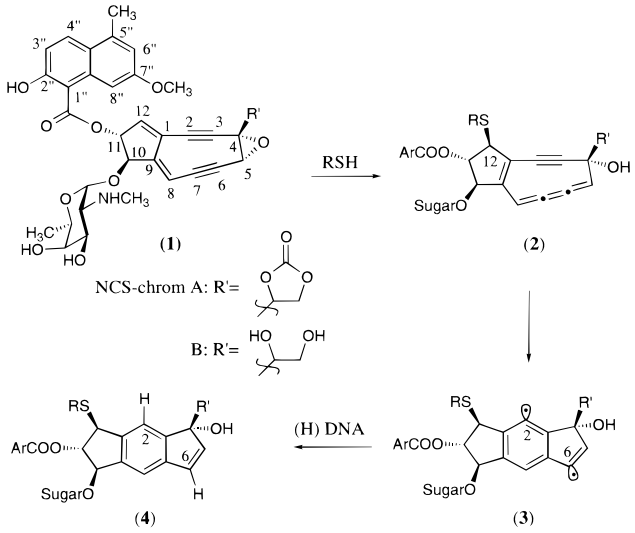

Under anaerobic conditions, NCS-chrom forms, instead, a covalent adduct linked to the deoxyribose moiety of the backbone of duplex DNA *(15)* or bulged DNA *(14, 16)*. Other potent enediyne antibiotics, such as C1027, have been recently found to produce drug-mediated interstrand cross-

† This work was supported by National Institutes of Health Grant GM 53793. Work at PNNL was supported as part of the Environmental Molecular Sciences Laboratory through the U.S. Department of Energy, Office of Biological and Environmental Research.

* To whom correspondence should be addressed.
‡ Harvard Medical School.
§ Pacific Northwest National Laboratory.

S0006-2960(97)02659-7 CCC: $15.00
Published on Web 01/22/1998

R11-D5 CACAGAAUUCG
gtctt

R11-D6 CACAGAAUUCG
gtgtct

R11-D7 CACAGAAUUCG
gtgtctt

R11-D8 CACAGAAUUCG
gtgtctta

R11-D9 CACAGAAUUCG
gtgtcttaa

R11-D11 CACAGAAUUCG
gtgtcttaagc

R11-R7 CACAGAAUUCG
GUGUCUU

D11'-D7 cacagaattcg
gtgtctt

D11'-R7 cacagaattcg
GUGUCUU

FIGURE 1: Sequences of RNA−DNA hybrid substrates. Uppercase represents RNA and lowercase indicates DNA. RNA overhangs are underlined.

links in addition to monoadducts in the absence of oxygen *(17, 18)*.

Since RNA−DNA hybrid structures play important roles in various biological processes, such as DNA replication, in gene transcription of chromosomal and mitochondrial DNAs, and during retroviral replication, it has been of interest to investigate these structures as substrates for the strand-cleaving enediynes. It has been found that glutathione-(GSH-) activated NCS-chrom generates double-stranded lesions in RNA−DNA hybrids due to selective C-1′ hydrogen abstraction on the RNA strand and C-5′ hydrogen abstraction at the DNA strand *(19)*. It was also observed, unexpectedly, that when four deoxyribonucleotides were deleted from the 5′ end of the DNA strand to create an RNA overhang, an apparently high molecular weight product with a very slow mobility was formed. Unlike most other DNA adducts and cross-linked products found previously, this material can be formed readily in the presence of atmospheric oxygen. In the present study, we show that the high molecular weight species is a monoadduct on the RNA strand of the RNA−DNA hybrid 5′-r(CACAGAAUU9CG)/5′-d(TTCTGTG) (R11−D7, Figure 1). This adduct is attached at the U9 position in the RNA strand and likely to the ribose of this nucleotide. The finding that the same amount of adduct is formed under aerobic and anaerobic conditions clearly demonstrates that formation of this RNA−drug monoadduct is not affected by molecular oxygen. This study broadens our view of the interaction between NCS-chrom and unusual nucleic acid structures and has implications for the possible effect of this antibiotic against viral RNA during its reverse transcription to DNA.

MATERIALS AND METHODS

Neocarzinostatin was purchased from Kayaku Antibiotics (Tokyo). NCS-chrom was extracted from the holoantibiotic following the published procedure *(20)*. The phosphoramidites and chemicals for the DNA synthesizer were from Glen Research. [γ-^{32}P]ATP and [5′-^{32}P]pCp were from New England Nuclear-DuPont. T4 polynucleotide kinase, T4 RNA ligase, and calf intestinal alkaline phosphatase were from New England Biolabs. The solutions and buffer for making polyacrylamide gels were from National Diagnostic. All other reagents were purchased from Fisher Scientific, Sigma, and Aldrich.

Synthesis and End-Labeling of Oligonucleotides. All DNA and RNA oligonucleotides were synthesized on an Applied Biosystems 381A DNA synthesizer. Synthesis of 5′,5′-dimethoxy-1′-deuterio-2′-*O*-(*t*-butyldimethylsilyl)uridine 3′-cyanoethyl phosphoramidite was as previously described *(19)*. 5′ Ends of oligonucleotides were labeled with [γ-^{32}P]-ATP and T4 polynucleotide kinase. 3′ Ends were labeled by T4 RNA ligase and [5′-^{32}P]pCp, as described *(21)*. The 3′-end-labeled oligonucleotides were dephosphorylated by calf intestinal alkaline phosphatase. The ^{32}P end-labeled oligonucleotides were purified on a 20% polyacrylamide gel.

Reaction of RNA−DNA Hybrid and NCS-Chrom. The RNA and DNA oligonucleotides were annealed by heating at 90 °C for 2 min and slowly cooled to room temperature. The reaction mixture contained 20−40 mM Tris-HCl (pH 8) and the desired amount of RNA−DNA hybrid. The reaction was initiated by addition of NCS-chrom and GSH (final concentration 1 mM) and proceeded for 1 h on ice in the dark. Samples were dried in a SpeedVac concentrator and resuspended in loading buffer and analyzed on 20% sequencing gels. The products were quantified by using a Molecular Dynamics PhosphorImager with Image Quant software.

The anaerobic reactions were carried in a Warburg vessel. The sidearm contained GSH and Tris-HCl (pH 8.0), while RNA−DNA hybrid and NCS-chrom in NaOAc (pH 5.8) were placed in the main chamber. The contents of the vessel were degassed by a freeze−evacuate−thaw procedure, as previously described *(22)*.

Gel Isolation and Sequencing of Adduct. The adduct, RNA, and DNA were separated on a 20% sequencing gel. The bands corresponding to the monoadduct were visualized by UV shadowing and excised from the gel. Adduct was eluted with water by following the crush and soak procedure. The 5′-end-labeled RNA oligonucleotides and RNA−drug adducts were analyzed by hydrolysis in sodium phosphate (pH 12) at 50 °C for 1 h or by RNase U2 digestion. Sequencing of the 3′-end-labeled RNA oligonucleotides and RNA−drug adducts was carried out by using chemical methodology. Hydrazine/H_2O (1:1) was used for U-specific modification, 3 M NaCl in hydrazine was used for C > U reaction, and diethyl pyrocarbonate (DEPC) was used for A > G modification, as described previously *(23)*. After chemical modification, the product was treated with 1 M aniline−HOAc (pH 4.5) at 60 °C for 20 min.

HPLC Isolation of Adduct. The adduct was gel-purified and then subjected to HPLC purification on a reverse-phase C-18 column. Buffer A was 0.1 M NH_4OAc (pH 6.5); buffer B was 50% acetonitrile and 0.05 M NH_4OAc. A gradient of 15−35% buffer B over a 40 min period was used for the separation. The elution was monitored by using Waters Type 486 UV (260 nm) and Type 474 fluorescence (excitation 340 nm, emission 420 nm) detectors. The HPLC fractions were collected and lyophilized for subsequent analysis.

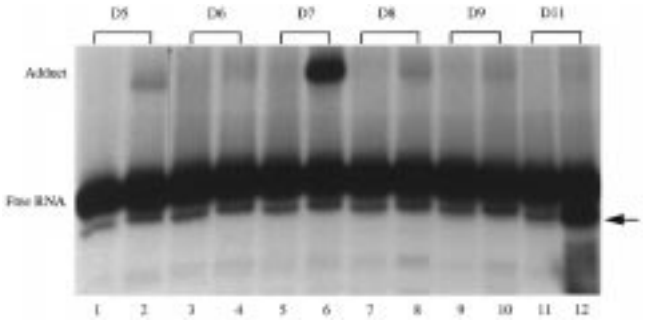

FIGURE 2: Slow mobility product formation depends on the length of the complementary DNA strand. RNA−DNA oligonucleotides (1:6.5) (28 μM) with 5′-^{32}P end-label on R11 were incubated with NCS-chrom (24 μM) in the presence and absence of GSH (1 mM). The DNA strand was varied. See Figure 1 for nomenclature. Lanes 1, 3, 5, 7, 9, and 11 are no GSH controls for lanes 2, 4, 6, 8, 10, and 12, respectively. The arrow indicates abasic site RNA product.

Mass Spectrometry. All MS experiments were performed with a 7 tesla electrospray ionization (ESI)−Fourier transform ion cyclotron resonance (FTICR) instrument, described in detail elsewhere *(24)*. ESI was performed in the positive ion mode with a sample flow of 200 nL/min *(25)*. Mass spectra were obtained utilizing standard experimental sequences employing selected ion accumulation with either broadband ($800 < m/z < 2500$; 20 Vpp) or single-frequency (1 Vpp) colored noise quadrupolar excitation waveforms *(26, 27)*. A piezoelectric pulse valve (Laser Techniques Inc., Albuquerque, NM) was used for gas introduction (N_2, ~10−5 Torr) for accumulated trapping of ions and for ion activation in collisionally induced dissociation (CID). Single-frequency dipolar off-resonance excitation, approximately 1 kHz higher than the reduced ion cyclotron resonance (ICR) frequency of the selected ion, was used for sustained off-resonance irradiation (SORI)−CID. The lyophilized HPLC fractions were reconstituted with 50 mM ammonium acetate (pH 7) and dialyzed against the same buffer using the microdialysis procedure described by Liu et al. *(28)* prior to ESI−FTICR analysis.

RESULTS AND DISCUSSION

Slow Mobility RNA Product Induced by Thiol-Activated NCS-Chrom. It has been reported previously that NCS-chrom induces damage in the form of abasic sites or cleavage on the RNA strand of a RNA−DNA hybrid in the presence of GSH due to 1′ chemistry at U8 or U9 of R11−D11 *(19)*. Interestingly, when the complementary DNA strand is shortened from its 5′ end, an apparently high molecular weight RNA product with a slow mobility on a denaturing polyacrylamide gel is observed. The formation of this product depends on the length of the corresponding DNA strand (Figure 2) and is formed most efficiently with D7 as the complementary DNA strand (Figure 2, lane 6). When additional nucleotides are added to the DNA strand, the slow mobility product diminishes, while abasic site damage (arrow) becomes predominant. Further shortening of D7 at its 5′ end (lane 4) also prevents the formation of the new product. However, when two nucleotides are removed from the 3′ end of D7 (lane 2), the formation of this product is still obvious, although much less, probably due to instability of duplex formation. Taken together, it appears that slow-mobility product formation with the hybrid requires a duplex region terminated by a four-ribonucleotide overhang at its 3′ end.

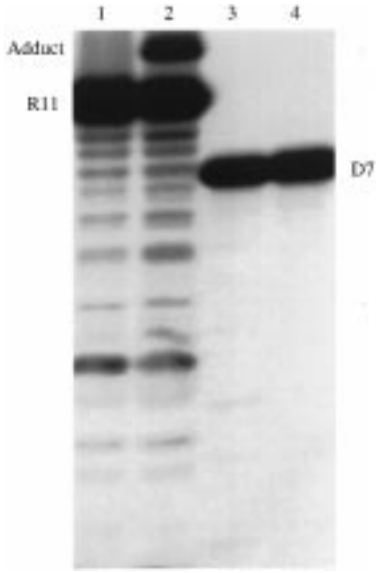

FIGURE 3: DNA strand is not involved in the slow mobility product. RNA−DNA hybrid R11−D7 (28 μM) with 5′-end-labeled R11 (lanes 1 and 2) or D7 (lanes 3 and 4) was treated with NCS-chrom (24 μM) in the absence (lanes 1 and 4) and presence (lanes 2 and 3) of 1 mM GSH.

Identification of the RNA−Drug Monoadduct. From its mobility characteristics, the new product might be either a drug−RNA adduct or RNA−DNA interstrand cross-linked material. The slow mobility product formed on R11−D7 induced by GSH-activated NCS-chrom was first characterized by labeling the 5′ end of the DNA strand D7. Since it is not detected when radiolabeled D7 in hybrid form R11−D7 was treated with GSH-activated NCS-chrom, the possibility of interstrand cross-linkage between R11 and D7 is excluded (Figure 3). Control reactions also indicate that it is not produced when R11 alone is incubated with NCS-chrom and glutathione (data not shown).

To obtain more direct evidence for drug adduct formation, the slow mobility product was separated from excess substrate and excised from the denaturing polyacrylamide gel, and its fluorescence was measured (Figure 4). The fluorescence spectrum of this material exhibits an excitation maximum at 345 nm and emission maximum at 425 nm, which is close to that of thiol-treated NCS-chromophore *(29)*, indicating that it is a drug adduct. A similar drug adduct band was observed when other thiols, such as cysteine (CYS), 2-mercaptoethanol (BME), and dithiothreitol (DTT) were used to activate NCS-chrom (Figure 5 A). About the same amount of adduct was formed with CYS, BME, and GSH, but DTT, which has two thiol groups, only produced $^1/_3$ the amount of adduct. This is different from the DNA adduct studied previously, which was formed most effectively with DTT as activator *(15)*. When 3-mercaptopropionate (MPA) is used to activate NCS-chrom, an adduct with a faster mobility than that activated by GSH is formed (Figure 5B). This demonstrates that thiol is also involved in the drug adduct, since the negatively charged MPA enhances its mobility on polyacrylamide gel.

Stability studies show that the drug adduct remains intact after heating at 90 °C or incubation with 1 M aniline−HOAc (pH 4.5) for 20 min (data not shown), indicating a covalent

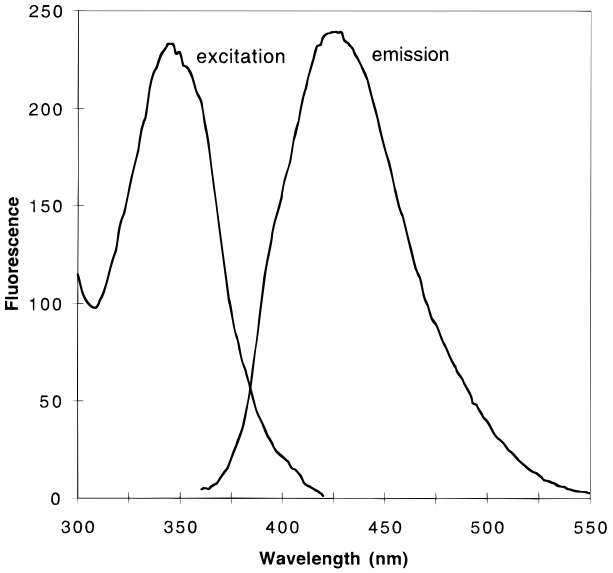

FIGURE 4: Fluorescence spectrum of purified slow mobility product. Fluorescence excitation was at 345 nm and emission was at 425 nm.

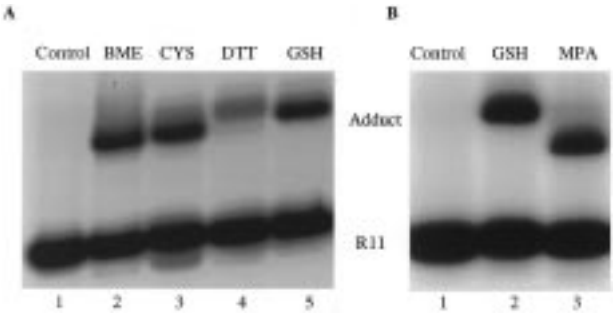

FIGURE 5: Involvement of thiol in the drug adduct. RNA−DNA hybrid (28 μM) with 5′-end-labeled R11 was treated with NCS-chrom (24 μM) and thiols. (A) Lane 1, no thiol control; lane 2, 1 mM BME; lane 3, 1 mM CYS; lane 4, 1 mM DTT; lane 5, 1 mM GSH. (B) Lane 1, no thiol control; lane 2, 1 mM GSH; lane 3, 1 mM MPA.

bonding between RNA and NCS-chrom and suggesting that linkage involves the sugar, not the base, of the RNA. Drug adducts isolated from polyacrylamide gel were further purified by HPLC. Two HPLC fractions with UV absorbance (260 nm) and fluorescence were isolated with elution times of 14.8 min (peak B) and 17.4 min (peak A) (Figure 6) and subsequently analyzed by ESI−FTICR MS. The observed molecular weights (MW_{obs}) of these two fractions are 4413.8 and 4439.8 Da, differing from that of intact R11 molecule (MW_{obs} = 3472.2 Da) by 968.6 ± 0.2 and 942.6 ± 0.2 Da, respectively. These differences correspond to the calculated molecular weights (MW_{calc}) of [rearranged NCS-chrom (A form) + GSH] (MW_{calc} = 968.3 Da) and [rearranged NCS-chrom (B form) + GSH] (MW_{calc} = 942.3 Da). The two fractions have a molecular weight difference of 26 Da, which can be generated from the conversion of NCS-chrom form A to B (*i.e.*, $-CO_2 + H_2O$) *(30)*. These data suggest that the RNA−drug adduct is a monoadduct that contains one form of NCS-chrom and glutathione.

Drug Attachment Site on RNA. To identify where NCS-chrom is attached to RNA, the monoadduct was isolated and sequenced with chemical methods. The drug position on RNA was first investigated by using 5′-end-labeled R11. The

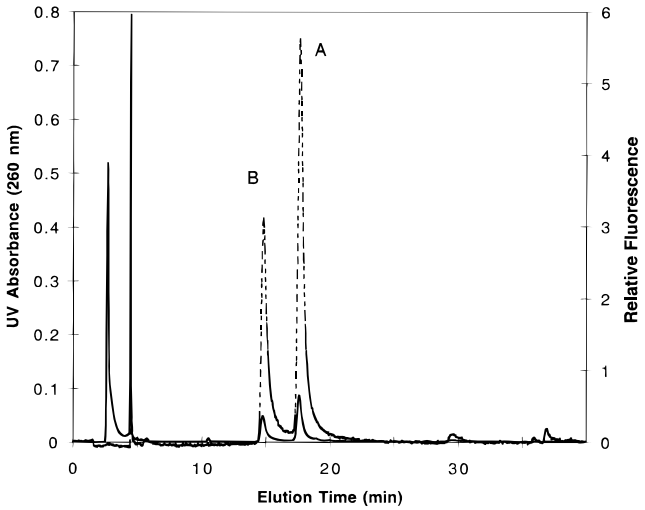

FIGURE 6: HPLC profile of RNA−drug adduct. Solid line represents UV absorbance at 260 nm, and dashed line indicates relative fluorescence. (A) Adduct of NCS-chrom form A; (B) adduct of NCS-chrom form B.

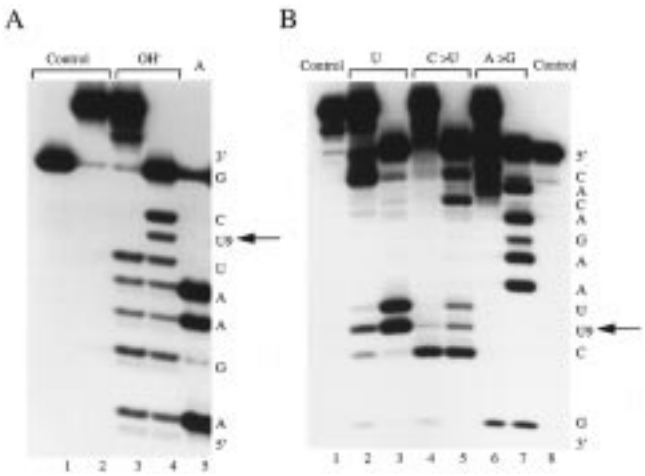

FIGURE 7: Chemical sequencing of monoadduct and intact R11. (A) Sequencing of the 5′-end-labeled R11 and the RNA adduct. Lane 1, R11 control; lane 2, adduct control; lane 3, alkaline hydrolysis ladder of monoadduct; lane 4, alkaline hydrolysis ladder of free R11; lane 5, A-specific R11 digestion with RNase U2. (B) Chemical sequencing of 3′-end-labeled R11 and monoadduct. Lane 1, adduct with aniline−HOAc (1 M) treatment control; lanes 2 and 3, U > C reaction for adduct and intact R11, respectively; lanes 4 and 5, C > U reaction for adduct and intact R11, respectively; lanes 6 and 7, DEPC-induced A > G reaction for drug adduct and intact R11, respectively; lane 8, R11 with aniline−HOAc treatment control.

alkaline hydrolysis ladder of drug adduct (Figure 7A, lane 3) is the same as that of intact 5′-end-labeled R11 (lane 4) up to U8. Alkaline hydrolysis of the RNA phosphate diester bond yields phosphate after each base at its 2′ or 3′ end. There is a gap beginning at U9 of the drug adduct hydrolysis ladder, indicating that NCS-chrom is attached to nucleotide U9. Monoadduct and free RNA with 3′-^{32}pCp end-label were also analyzed by base-specific chemical sequencing. The bases were modified specifically by hydrazine or DEPC, followed by aniline−HOAc treatment to induce base-specific RNA cleavage. The observed 3′-end-labeled fragments lack the sugar of the modified base and have phosphate at their 5′ ends (Figure 7B). The U lane for drug adduct shows that the band at U9 is normal, but the U8 band is presumably

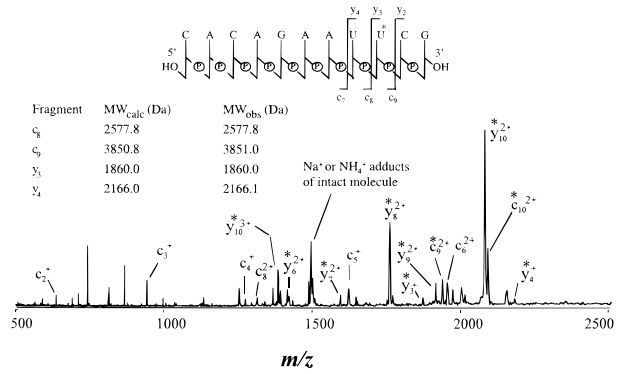

FIGURE 8: SORI−CID analysis of the late eluting (17.4 min) HPLC fraction. The peak assignments are based on the nomenclature from ref *31*; c represents an ion containing the 5′-OH group, and y represents an ion containing the 3′-OH group. Asterisks indicate fragments containing intact drug molecule. (Inset) Calculated and observed molecular weights of four fragments, allowing the determination of the drug attachment site as U9.

retarded (lane 2). C > U and A > G sequencing reactions show that the bands of the bases above U9 also have slower mobilities than those of intact RNA (lanes 4 and 6), confirming that U9 is the attachment site. By combining the results with 3′- and 5′-end-labeled RNA, it is clear that U9 is the only drug attachment site.

The drug attachment site was further confirmed by SORI−CID MS/MS analysis of the drug monoadduct. After isolation in the ICR cell, the intact drug adduct ions were subjected to collisionally induced dissociation. As shown in Figure 8, abundant fragment ions were observed from the late-eluting fraction (17.4 min). The intact drug adduct was observed for all fragments incorporating U9, indicating that the drug is covalently bound to RNA, since noncovalent associations will not survive the SORI−CID process, and further confirming the stability study results. Similar results were also obtained from the early-eluting fraction (14.8 min) and a mass difference of 26 Da was only observed in the drug-containing fragments, compared with those from the late-eluting fraction (17.4 min). These results are again consistent with the solution studies, suggesting that the two adducts isolated from HPLC are from two forms of NCS-chrom, and they are covalently attached to U9 exclusively.

Atmospheric O_2 Does Not Inhibit Formation of RNA−Drug Monoadduct. The enediyne drugs were found to form stable covalent monoadducts with DNA duplex mainly under anaerobic conditions *(14, 15, 17)*. In our system, drug adduct is also readily formed under aerobic conditions. The reaction was performed in the presence and absence of oxygen, as described in Materials and Methods, and the yield of monoadduct (drug:hybrid = 2) formed was quantified by the PhosphorImager. A yield of 17% drug monoadduct was obtained when oxygen was depleted, and the same amount of RNA−drug adduct was formed under aerobic conditions (subjected to the same freeze and thaw procedures as the anaerobic sample). Product formation is roughly linear up to a drug:hybrid ratio of 4.

In the previous study, it was found that the NCS-chrom diradical **3** (Scheme 1) abstracted H from C-1′ of U8 or U9 on R11 of R11−D11, and the resulting RNA radical undergoes O_2-dependent degradation to produce an abasic site or RNA fragmentation *(19)*. It is possible that drug adduct formation and oxidative sugar damage have a common RNA

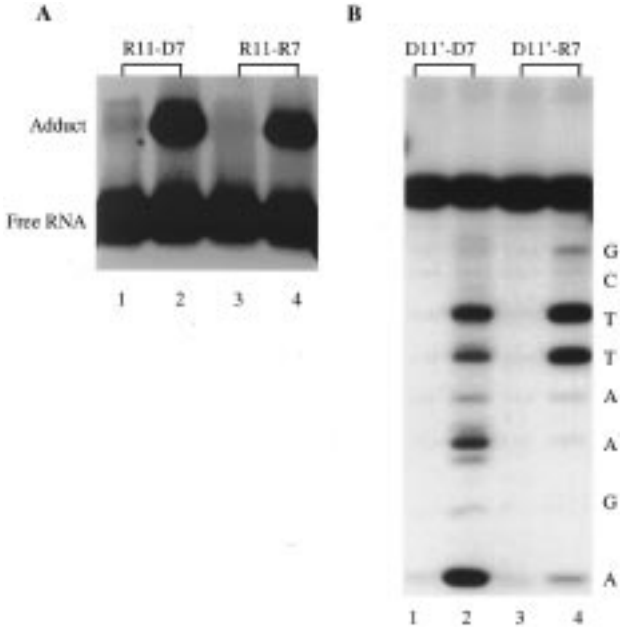

FIGURE 9: Substitution of R11 in R11−D7 with its DNA analogue D11′ leads to strand scission. See Figure 1 for nomenclature. (A) Adduct formation of RNA−DNA hybrid R11−D7 and RNA duplex R11−R7 with 5′-end-labeled R11 induced by NCS-chrom (24 μM). Lanes 1 and 3, no GSH control; lanes 2 and 4, with GSH (1 mM) activation. (B) Cleavage of DNA duplex D11′−D7 (lanes 1 and 2) and RNA−DNA hybrid D11′−R7 (lanes 3 and 4) with 5′-end-labeled 11-mer DNA induced by NCS-chrom (24 μM). Lanes 1 and 3, no GSH control; lanes 2 and 4, with GSH (1 mM) activation.

radical intermediate. The carbon-centered RNA radical formed after H abstraction by diradical **3** might spontaneously add back onto GSH-activated NCS-chrom to form the observed RNA−drug monoadduct. It is clear that the hybrid R11−D7 binds thiol-activated NCS-chrom with the orientation and distance geometry that favor the selective formation of the monoadduct, instead of the oxidative damage products (abasic site or break). Therefore, the rate of this reaction is much greater than the competitive reaction, which eventually leads to strand scission or abasic site formation ($k_2 \gg k_3$). Consequently, drug adduct becomes the major product.

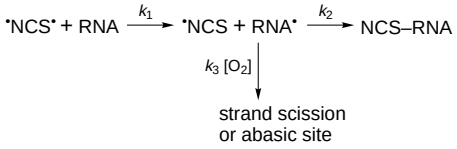

Substitution of R11 with DNA Leads to Strand Scission. When D7 in hybrid R11−D7 is replaced with a RNA strand with the same sequence, the resulting RNA duplex R11−R7 (Figure 1) forms a similar drug adduct as that of hybrid R11−D7 (Figure 9A, lanes 2 and 4). However, the yield of RNA duplex appears to be slightly lower than that of the RNA−DNA hybrid (lane 2), perhaps caused by the difference of binding affinity of NCS-chrom for RNA−RNA and RNA−DNA duplexes. When R11 of R11−D7 is replaced with a DNA strand to give DNA duplex D11′−D7 (Figure 1), this DNA strand (top strand) has strand scission at A4, A6, A7, T8, and T9 instead of adduct formation (Figure 9B, lane 2). The cleavage pattern is similar to that of the fully complementary DNA duplex *(19)*. Substitution of D7 (bottom strand) in this DNA duplex with the RNA strand

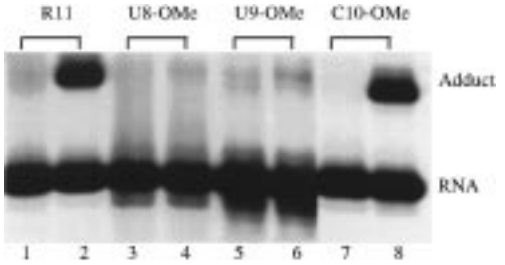

FIGURE 10: Effect of 2′-O-methyl substitution on adduct formation. 5′-^{32}P-End-labeled R11 (lanes 1 and 2), 5′-r(CACAGAAU$_{OMe}$UCG) (lanes 3 and 4), 5′-r(CACAGAAUU$_{OMe}$CG) (lanes 5 and 6), or 5′-r(CACAGAAUUC$_{OMe}$G) (lanes 7 and 8) in hybrid form (28 μM) were treated with NCS-chrom (24 μM) as described in Materials and Methods. Lanes 1, 3, 5, and 7, no GSH controls; lanes 2, 4, 6, and 8, with GSH (1 mM) activation.

5′-r(UUCUGUG) protects the nucleotides in the duplex region; only T8 and T9 in the single-stranded region of hybrid D11′−R7 (Figure 1) are cleaved (Figure 9B, lane 4). The number of cleavage sites is less in the RNA−DNA hybrid than in the duplex DNA, probably because of their different drug binding characteristics. But interestingly, NCS-chrom still can bind to the end of the RNA−DNA duplex and induce the cleavage at T8 and T9 of the single-stranded region (lane 4). Replacement of the four-base overhang r(UUCG) of hybrid R11−D7 with a 4-deoxyribonucleotide terminus [d(TTCG)] virtually entirely eliminates monoadduct formation (data not shown). Adduct formation involving the RNA overhang may reflect the known ability of RNA to adopt various three-dimensional structures. The single-stranded region of RNA may wrap around the drug and form a binding pocket that favors adduct formation.

Effect of 2′-O-Methyl and 2′-H Substitution on Adduct Formation. Substitution of U8 or U9 with 2′-*O*-methyluridine dramatically inhibits drug adduct formation (Figure 10, lanes 4 and 6), but substitution of C10 with 2′-O-methylcytidine has no obvious effect (lane 8). NCS-chrom is believed to intercalate normal DNA duplex with its naphthoate moiety, and the rest of the molecule binds to the DNA minor groove. In the RNA−DNA hybrid with a single-strand RNA tail, the binding mode of NCS-chrom is likely quite different from that with duplex DNA. NCS-chrom probably intercalates its naphthoate moiety into or stacks at the end of the duplex region of RNA−DNA hybrid next to the RNA overhang with the rest of the molecule hugging the four-base overhang region of the RNA strand. Therefore, changing 2′-OH to the bulky 2′-O-methyl group at U8 or U9, which are at or close to the binding site, would be expected to affect the binding of NCS-chrom to the hybrid and cause the decrease of drug adduct yield. The 2′-O-methyl group at U9 also may make it impossible for the drug to attach to this nucleotide. The 2′-O-methyl group at C10, which may not be involved directly in binding, has no obvious effect on adduct formation. Substitution of U8 or U9 with deoxyuridine inhibits adduct formation about 80% (Table 1, substrates 2 and 3). This suggests that the 2′-OH groups of U8 and U9, which are likely to be involved in forming a proper three-dimensional binding structure, are required for adduct formation.

Nucleotide Substitution and Mechanism of the Reaction. The composition of the four-base overhang region of the RNA strand plays a very important role in adduct formation.

Table 1: Effect of Nucleotide Substitution on Monoadduct Formation[a]

substrate	RNA−DNA hybrid	monoadduct formation (%)
1	CACAGAAUUCG gtgtctt	100
2	CACAGAAU<u>u</u>CG gtgtctt	17
3	CACAGAA<u>u</u>UCG gtgtctt	17
4	CACAGAA<u>C</u>UCG gtgtctt	13
5	CACAGAA<u>t</u>UCG gtgtctt	20
6	CACAGAA<u>A</u>UCG gtgtctt	4
7	CACAGAAU<u>G</u>CG gtgtctt	14
8	CACAGAAU<u>A</u>CG gtgtctt	39

[a] ^{32}P-End-labeled RNA in the indicated hybrid (28 μM) was treated with GSH- (1 mM) activated NCS-chrom (24 μM) as described in Materials and Methods. Lowercase letters denote deoxyribo residues, and substituted nucleotides are underlined. Yield of monoadduct was calculated relative to that of R11−D7 (substrate 1).

Changing certain bases greatly inhibits adduct formation. Nucleotide substitution of U8 by A inhibits adduct formation almost completely, but substitution of U8 with C or T still allows about 20% adduct formation (Table 1, substrates 4−6). It appears that a pyrimidine has to be at this position for a certain amount of drug adduct to form. Changing U9 to a purine results in decreased but still significant product formation (Table 1, substrates 7 and 8). Hybrids with extension of the overhang RNA region by additional nucleotides decrease the drug monoadduct yield; the longer the oligonucleotide addition, the less the adduct formation (Table 2, substrates 2 and 3). This result suggests that the added nucleotides distort the binding pocket of the RNA−DNA duplex with NCS-chrom to different extents. But even the single nucleotide deletion of G or C from the 3′ end of the overhang eliminates adduct formation completely (substrates 4 and 5). When G11 is replaced with A or C, virtually no detectable adduct is formed, but substitution with inosine still allows formation of a small amount of adduct (substrates 6−8). This suggests that guanine O6 plays an important role and that the 2-amino group is also involved in adduct formation, possibly aiding binding of the activated drug by the RNA−DNA hybrid through H-bonding with either the drug or another nucleotide.

It was found previously that thiol-activated NCS-chrom diradical **3** (Scheme 1) abstracts hydrogen from C-1′ of U8 or U9 on the RNA strand of the fully complementary RNA−DNA hybrid (*19*). The resulting carbon-centered RNA radical produces oxygen-dependent degradation products. It is possible that the adduct formation reaction has a similar RNA radical intermediate. To address this question, 5′-^{32}P-end-labeled R11 containing deuterium at the C-1′ position of U8 or U9 in R11−D7 was treated with GSH-activated NCS-chrom. The yield of adduct formed with the two

Table 2: Effect of Nucleotide Substitution on Monoadduct Formation[a]

substrate	RNA−DNA hybrid	monoadduct formation (%)
1	CACAGAAUUCG gtgtctt	100
2	CACAGAAUUCGC gtgtctt	77
3	CACAGAAUUCGCACCAG gtgtctt	60
4	CACAGAAUUC gtgtctt	not detected
5	CACAGAAUUG gtgtctt	not detected
6	CACAGAAUUCA gtgtctt	not detected
7	CACAGAAUUCI gtgtctt	20
8	CACAGAAUUCC gtgtctt	3

[a] Conditions and analysis are the same as in Table 1.

deuterium-substituted substrates was quantified and compared with that of protium-containing R11−D7, but no obvious isotope effect was detected for U8 (H/D = 1.1) or U9 (H/D = 0.9).

CONCLUDING REMARKS

In the present study we show the RNA strand of an RNA−DNA hybrid forms a monoadduct with NCS-chrom in the presence of thiol. The drug adduct is formed only when the DNA strand is shorter than its complementary RNA strand. Under the same conditions, the fully complementary RNA−DNA duplex produces only RNA degradation products. The drug is attached to the U9 position, probably on the ribose of this nucleotide. Since the DNA is hydrogen-bonded to one of the Us that is damaged in the fully complementary duplex, it is possible that the binding mode of the adduct-producing complex is similar to that of the fully complementary duplex, with the naphthoate moiety of NCS-chrom intercalating into or stacking on the existing RNA−DNA duplex. This possibility is supported by the observation that further truncation of the DNA strand from its 5′ end prevents adduct formation, but truncation at the 3′ end still results in production of a small amount of adduct. Unlike fully complementary RNA−DNA hybrid that positions the drug in its minor groove, due to the ability of single-stranded RNA to assume unusual three-dimensional structures, the flanking RNA overhang may wrap around NCS-chrom to form a tight binding pocket. Substitution of 2′-OH with the bulky 2′-O-methyl group on U8 presumably hinders the binding of GSH-activated NCS-chrom to the structure formed by RNA and prevents adduct formation. The sequence of the RNA overhang and the presence of the A−T-rich duplex region next to it are essential for adduct formation, presumably by generating an appropriate three-dimensional binding structure.

Unlike most other stable enediyne adducts, this RNA−drug adduct can be formed at the same yield under aerobic or anaerobic conditions. This may be the result of the much greater rate of adduct formation relative to the oxidative degradation of the RNA, which leads to abasic site formation and strand scission ($k_2 \gg k_3$). Again, this may reflect the snug binding and critical placement of the drug in the binding pocket.

The significance of the absence of an isotope effect on adduct formation with substrate possessing deuterium instead of protium at the C-1′ of U9 is unclear. A substantial isotope effect ($k_H/k_D = 3.2$) has been found in the NCS-induced formation of strand breakage and abasic sites at this nucleotide (as well as at U8) in the fully complementary hybrid substrate *(19)*. While these latter results imply that adduct formation may not involve C-1′ hydrogen abstraction, it must be noted that deuterium isotope selection effects have not been found in hydrogen abstraction reactions by certain other enediyne antibiotics, such as calicheamicin *(32)* and esperamicin *(33)*, whereas they have been with NCS *(34, 35)* and C-1027 *(36)*. Further, such isotope effects have been founded to vary substantially with the sequence adjacent to the target site *(34, 35)*. Also, to realize a kinetic isotope effect, it is necessary that activated-drug binding has a significant off-rate component. If binding is essentially irreversible, no isotope effect would be expected. Additionally, as noted above, the snugness of the fit of the drug at its binding site may limit the ability of dioxygen to compete for the carbon-centered radical generated on the DNA. Accordingly, the absence of an isotope effect cannot be taken as proof that hydrogen atom abstraction does not occur at C-1′ of U9. Nevertheless, it remains possible that another site on the sugar moiety of U9 (or even its base) is the source of the abstracted hydrogen. While hydrogen abstracted by all enediynes studied to date has come from the sugar, it has not been ruled out that in the unusual structure, which is likely generated by the RNA overhang, it is the base at U9 that is attacked by the activated drug. The stability of the adduct to treatment with aniline−acetic acid, however, makes the latter unlikely. These various considerations require further investigation.

REFERENCES

1. Goldberg, I. H., and Kappen, L. S. (1995) in *Enediyne Antibiotics as Antitumor Agents* (Borders, D. B., and Doyle, T. W., Eds.) pp 327−362, Dekker, New York.
2. Goldberg, I. H. (1991) *Acc. Chem. Res. 24*, 191−196.
3. Xi, Z., and Goldberg, I. H. in *Comprehensive Natural Products Chemistry* (Barton, D. H., and Nakanishi, K., Eds.) Elsevier Science, Oxford, England (in press).
4. Napier, M. A., Holmquist, B., Strydom, D. J., and Goldberg, I. H. (1981) *Biochemistry 20*, 5602−5608.
5. Gao, X., Stassinopoulos, A., Rice, J. S., and Goldberg, I. H. (1995) *Biochemistry 34*, 40−49.
6. Dasgupta, D., and Goldberg, I. H. (1985) *Biochemistry 24*, 6913−6320.
7. Povirk, L. F., Dattagupta, N., Warf, B. C., and Goldberg, I. H. (1981) *Biochemistry 20*, 4007−4014.
8. Hensens, O. D., and Goldberg, I. H. (1989) *J. Antibiot. 42*, 761−768.
9. Myers, A. G. (1987) *Tetrahedron Lett. 28*, 4493−4496.
10. Myers, A. G., Proteau, P. J., and Handel, T. M. (1988) *J. Am. Chem. Soc. 110*, 7212−7214.
11. Kappen, L. S., and Goldberg, I. H. (1993) *Science 261*, 1319−1321.
12. Kappen, L. S., and Goldberg, I. H. (1993) *Biochemistry 32*, 13138−13145.
13. Kappen, L. S., and Goldberg, I. H. (1995) *Biochemistry 34*, 5997−6002.

14. Kappen, L. K., Xi, Z., and Goldberg, I. H. (1997) *Bioorg. Med. Chem. 5*, 1221−1227.
15. Povirk, L. F., and Goldberg, I. H. (1984) *Biochemistry 23*, 6304−6311.
16. Kappen, L. K., and Goldberg, I. H. (1997) *Biochemistry 36*, 14861−14867.
17. Xu, Y. J., Zhen, Y. S., and Goldberg, I. H. (1997) *J. Am. Chem. Soc. 119*, 1133−1134.
18. Xu, Y.-j., Xi, Z., Zhen, Y. S., and Goldberg, I. H. (1997) *Biochemistry 36*, 14975−14984.
19. Zeng, X., Xi, Z., Kappen, L. S., Tan, W., and Goldberg, I. H. (1995) *Biochemistry 34*, 12435−12444.
20. Myers, A. G., Cohen, S. B., and Kwon, B.-M. (1994) *J. Am. Chem. Soc. 116*, 1670−1682.
21. England, T. E., Bruce, A. G., and Uhlenbeck, O. C. (1980) *Methods Enzymol. 65*, 65−74.
22. Kappen, L. S., and Goldberg, I. H. (1985) *Nucleic Acids Res. 13*, 1637−1648.
23. Peattie, D. A. (1979) *Proc. Natl. Acad. Sci. U.S.A. 76*, 1760−1764.
24. Winger, B. E., Hofstadler, S. A., Bruce, J. E., Udseth, H. R., and Smith, R. D. (1993) *J. Am. Soc. Mass Spectrom. 4*, 566−577.
25. Gale, D. C., and Smith, R. D. (1993) *Rapid Commun. Mass Spectrom. 7*, 1017−1021.
26. Bruce, J. E., Anderson, G. A., Hofstadler, S. A., Vanorden, S. L., Sherman, M. G., Rockwood, A. L., and Smith, R. D. (1993) *Rapid Commun. Mass Spectrom. 7*, 914−919.
27. Bruce, J. E., Vandorden, S. L., Anderson, G. A., Hofstadler, S. A., Sherman, M. G., Rockwood, A. L., and Smith, R. D. (1995) *J. Mass Spectrom. 30*, 124−133.
28. Liu, C., Wu, Q., Harms, A. C., and Smith, R. D. (1996) *Anal. Chem. 68*, 3295−3299.
29. Povirk, L. F., and Goldberg, I. H. (1986) *Nucleic Acids Res. 14*, 1417−1426.
30. Napier, M. A., Goldberg, I. H., Hensens, O. D., Dewey, R. S., Liesch, J. M., and Albers-Schonberg, G. (1981) *Biochem. Biophys. Res. Commun. 100*, 1703−1712.
31. Ni, J., Pomerantz, S., Rozenski, J., Zhang, Y., and McCloskey, J. (1996) *Anal. Chem. 68*, 1989−1999.
32. De Voss, J. J., Townsend, C. A., Ding, W.-D., Morton, G. O., Ellestad, G. A., Zein, N., Tabor, A. B., and Schreiber, S. L. (1990) *J. Am. Chem. Soc. 112*, 9669−9670.
33. Kozarich, J., Worth, L., Frank, B. L., Christner, D. F., Vanderwall, D. E., and Stubbe, J. (1989) *Science 245*, 1396−1399.
34. Kappen, L. S., Goldberg, I. H., Wu, S. H., Stubbe, J., Worth, L., Jr., and Kozarich, J. W. (1990) *J. Am. Chem. Soc. 112*, 2797−2798.
35. Frank, B. L., Worth, L., Jr., Christner, D. F., Kozarich, J. W., Stubbe, J., Kappen, L. S., and Goldberg, I. H. (1991) *J. Am. Chem. Soc. 113*, 2271−2275.
36. Xu, Y. J., Xi, Z., Zhen, Y. S., and Goldberg, I. H. (1995) *Biochemistry 34*, 12451−12460.

BI972659W